DEVELOPMENT, TESTING AND SIMULATION BASED OPTIMIZATION OF A SPLIT-TYPE HEAT PUMP FOR MINIMAL INVASIVE RENOVATION OF BUILDINGS

William Monteleone[1], Fabian Ochs[1], Samuel Breuss[1], Christof Drexel[2]
[1] *University of Innsbruck, Austria, E-Mail: william.monteleone@uibk.ac.at*
[2] *drexel reduziert GmbH, Bregenz, Austria, E-Mail: c.drexel@drexelreduziert.at*

Abstract

Buildings play a crucial role in the decarbonisation of the energy consumption. In refurbished multi-family buildings, the substitution of centralized fossil-based heating systems is not always convenient for techno-economical reasons. On the other hand, decentral systems which require minimal invasive construction works are not offered on the market and frequently, especially for domestic hot water preparation, gas burners or inefficient electrical boilers are mounted in single apartments. Through coupled simulation and measurement work, a façade-integrated split air-to-water micro heat pump was developed and proposed as an efficient and sustainable alternative to fossil-based technologies.

Introduction

Improving the energy performance in the building sector is crucial for a clean energy transition. Buildings, in fact, account for about 40 % of the final energy consumption and 36% of greenhouse gas emissions in Europe (European Commission, 2019). In addition to that, several countries within the European Union will begin banning oil and gas-fired boilers starting from 2024. In Austria oil and gas boilers will be banned in all buildings from 2050 on while in Germany only oil boilers will be banned in all buildings by the same time (Environmental Coalition on Standards, 2021). Therefore, it is of extreme importance to increase the adoption of sustainable and efficient technologies for the supply of heating, domestic hot water and eventually cooling in buildings. Heat pumps are nowadays widely regarded as a key technology for the electrification of space and water heating (IEA, 2021a) and thus reach a full decarbonisation of the building sector by 2050, as prescribed by the EPBD (European Commission, 2018). In refurbished buildings, particularly in urban areas, it is often not possible to upgrade or substitute an existing centralised heating system for several technical, economic and social reasons. Therefore, due to the lack of alternatives, decentralised gas-fired systems for heating and/or domestic hot water preparation are still prevalent, alongside electrical boilers (IEA, 2020). As stricter regulations regarding the building envelope contribute to a substantial reduction in the heating demand, the domestic hot water demand stays constant independently from the type of residential building. Accordingly, the market does not provide solutions for a flat-wise domestic hot water preparation, which are modular, silent and, at the same time, require minimal invasive construction work. District heating networks remain a valid option for many densely populated areas where the installation of a heat pump is impractical but their accessibility remains limited to relatively large urban centres (IEA, 2021b). Given the current state-of-the-art, a façade-integrated mini-split air-to-water heat pump was designed and optimized by means of CFD and refrigerant cycle simulations. At the conclusion of a preliminary design, a real-scale functional model of the heat pump was produced and tested in laboratory. In parallel, dynamic systems simulations were performed to assess the system performance depending on different water drawing profiles (according to (DIN EN 16147:2017)).

Concept

The developed design features a façade-integrated element housing the evaporator and four axial fans. Serviceability is provided via a double panel system which can be accessed externally from the façade, without the need of entering the flat for maintenance. On the other end, the indoor element includes the remaining components of the heat pump cycle, as well as the domestic hot water storage, a freshwater station for the delivery of domestic hot water and the necessary hydraulic components for water circulation. The entire element comes in a compact and space saving fashion and can be easily mounted in the bathroom in the space over a washing machine, thus not requiring floor surface or cooling down ambient air (e.g. as in the case of ambient air domestic hot water heat pumps).

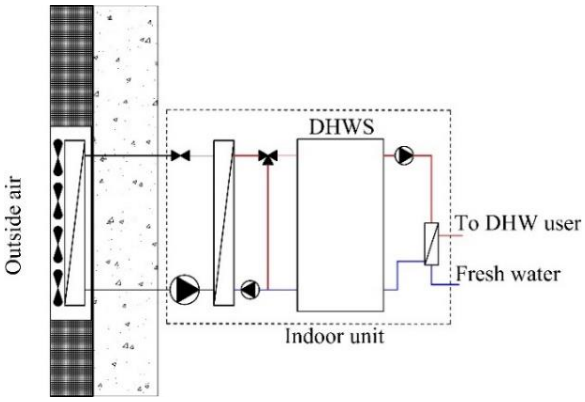

Figure 1: Conceptual design of a façade-integrated mini-split heat pump for the supply of domestic hot water.

No particular regulations regarding Legionella apply in this case, since hot water is not directly delivered to the user from the storage but instead through a freshwater station. The heat pump cycle runs on propane (R290), one of the long-term sustainable refrigerants (ref. annex 50) due to its low Global Warming Potential (GWP). Its high flammability constrains, however, the maximum refrigerant charge to 150 g for heat pump units installed indoors. Several storage sizes (from 90 to 120 liters) were investigated and evaluated by means of dynamic system simulation.

Simulation and experiment

Firstly, the optimal design of the façade-integrated element was investigated by means of CFD simulations based on overall pressure drop and flow homogeneity. Secondly, the overall performance of the refrigerant cycle was assessed through steady-state refrigerant cycle simulations and laboratory measurements. Then, dynamic system simulations were performed with the aim of analysing the system performance for defined water drawing profiles on daily and yearly basis.

CFD-based design optimization

Façade-integration and a compact layout demand a deep investigation of the fluid dynamics within the outdoor element. Not only is the minimisation of the overall pressure drop a key factor, but also the homogeneity rate of the flow pattern since it can directly affect the evaporation pressure and thus the overall performance of the refrigerant cycle. Therefore CFD simulations were performed to determine the optimal design of the outdoor unit within the software environment of *Ansys 19.2*. Flow homogeneity in different evaporator-fan configurations was evaluated, in first approximation, in terms of standard deviation as follows:

$$\sigma_{flow,\%} = \frac{\sqrt{\left[\left(v_{vol} - v_{x,y}\right)^2\right]}}{v_{vol}} \cdot 100 \qquad (1)$$

with v_{xy} being the velocity distribution and v_{vol} the volume-averaged velocity. Since the modelling of air passages in plate-fin heat exchangers is complex, the evaporator was modelled as a porous solid with defined streamwise and transverse loss coefficients, calibrated to match the pressure drop observed in the laboratory measurements. A k-ε turbulence model was used, due to its extensive application in flow patterns around baffles and rotating domains (e.g. the fans) and its improved accuracy compared to other turbulence models (Abeykoon, 2020). Table 1 summarizes the assumptions adopted for each simulation variant:

Table 1: Boundary conditions adopted for each CFD simulation.

Position	Boundary condition
Inlet	Total pressure = 0 Pa
Outlet	Mass flow = 0.10 kg/s
Walls	No Slip Wall (friction model)
Evaporator	Streamwise loss coeff. = 363 m^{-1}
Evaporator	Transverse loss coeff. = 3630 m^{-1}

The analysis considered designs with both axial and radial fans.

Refrigerant cycle simulation

Steady-state refrigerant cycle simulations were performed with the aim of investigating the maximum theoretical performance of a propane-based refrigerant cycle at given boundary conditions (e.g. air and water volume flows). For sake of semplicity and to avoid numerically expensive procedures, the airflow pattern was considered fully uniform and therefore any flow inhomogeneity will not be part of this discussion. The refrigerant cycle model follows a modular semi-physical approach, meaning that for each component of the refrigerant cycle (in this case compressor, condenser, expansion valve and evaporator) at least one equation is used to fully characterize the heat transfer or the refrigerant mass flow rate.

The refrigerant mass flow rate supplied by a reciprocating compressor is expressed, depending on the rotational speed, by the following equation:

$$\dot{m}_{ref} = \eta_{vol} \frac{n_{rpm}}{60} D_c \rho_{ref,suction} \qquad (2)$$

With:

η_{vol} : Volumetric efficiency

n_{rpm} : Rotational speed of the compressor in [rpm]

D_c : Displacement of the compressor in [m^3]

$\rho_{ref,suction}$: Refrigerant suction gas density in [kg/m^3]

The calculation of the refrigerant mass flow requires thus the knowledge about the evolution of the volumetric efficiency at different compression ratio. One possibility could be to derive a curve linking the volumetric efficiency to the pressure conditions inside the compressor from literature data or measurements from similar compressor (same technology, similar displacement volume). Another one, which in the end was adopted, is to implement a theoretical model such as:

$$\eta_{vol} = 0.97 - \left[\left(\frac{z_s}{z_d}\right)\tau^{\frac{1}{k}} - 1\right] C_l - e_v \qquad (3)$$

Where:

z_s : Compressibility factor of the refrigerant at suction side

z_d : Compressibility factor of the refrigerant at discharge side

τ : Compression ratio

k : Isentropic expansion factor

C_l : Clearance volume of the compressor (dead volume) in [m^3]

e_v : Correction coefficient

As a first approximation, thermal losses are attributed solely to the compressor. The loss through the compressor shell is expressed by the following relationship:

$$\dot{Q}_{loss} = UA_{compr}\left(\vartheta_{compr} - \vartheta_{amb}\right) \qquad (4)$$

Being:

UA_{compr} : Compressor shell overall heat transfer coefficient in [W/K]

ϑ_{compr} : Compressor shell temperature

ϑ_{amb} : Temperature of the technical room

For sake of simplicity, the expansion valve was simply modelled as isenthalpic for which:

$$h_{exv,in} = h_{exv,out} \qquad (5)$$

The refrigerant cycle model iterates on the heating and cooling power (respectively at the condenser and at the evaporator) to fully characterize the refrigerant cycle. The adopted convergence criteria checks if the overall balance of the heat pump is satisfied as well as proving the validity of the energy balance for the single components of the model. The output of the refrigerant cycle model is a series of performance maps of the heating and electric power, depending from source and sink temperatures, which will be given as an input to the dynamic model taking into account water drawing profiles. Performance maps were generated for 5, 10, 15 and 20 °C air inlet temperatures and 30, 40, 50 °C water supply temperatures.

Dynamic system simulation

In order to evaluate the efficiency and functionality of the entire system when supplying the DHW demand, a dynamic model was created within the simulation environment of *MATLAB* and *Simulink* with the additional use of the CARNOT toolbox (Solar-Institut Juelich FH Aachen, 2018). The heat pump was implemented in a simplified way using a LookUp Table (from the results of the refrigerant cycle simulation). The dynamic performance of the system was evaluated at the source temperature conditions indicated by the standard EN 14511 (DIN EN 14511-2:2018), that is -10, -7, 2, 7 , 12 °C with the addition of a point at 20 °C to take into account for summer operation. For source temperatures lower than 5 °C (not provided in the generated look-up tables), the heating power and the corresponding coefficient of performance are extrapolated linearly. Four different storage tank sizes were simulated, corresponding to 90, 100, 110 and 120 liters.

Minimum and maximum operational time intervals were assigned to the heat pump model. In order to take deicing operation into account in a simplified way, a shortened operating interval is assumed for source temperatures between -7 and 7 °C. However no additional electric power consumption was modelled to this moment. At source temperatures lower than -7 °C the reduced humidity content of air makes ice formation less likely and no deicing operation was assumed in these cases.

For the evaluation of the yearly performance factor (SPF), daily-averaged temperature data for an entire year for the city of Innsbruck, Austria were selected.

For space and installation reasons, the height of the storage tank was assumed to be constant and equal to 1.1 m, while the diameter of the tank increases with increasing volume. A different insulation thickness was selected for each storage volume to always fit an energy efficiency class of ErP B.

The ambient temperature, which serves as a boundary condition for the losses of the individual components, was assumed as constant and equal to 20 °C.

The freshwater station (heat exchanger), mixing valves, pipes and circulation pumps were also simulated with specific components from the

CARNOT toolbox. The pipe lengths correspond to the lengths in the experimental setup.

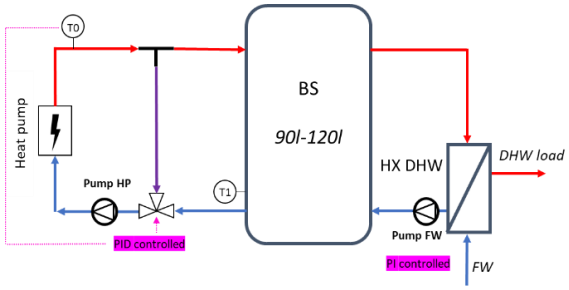

Figure 2: Schematic representation of the modelled hydraulic layout and indication of controls used for the dynamic system simulations.

By means of a fixed value control, the storage tank is charged at a fixed temperature (52°C). In the start-up phase of the heat pump, the temperature of the water supplied to the storage tank is lower than the storage temperature. If no additional measure was undertaken, this would have a detrimental effect on the system performance, interfering with the stratification of the storage tank. For this reason, during the start-up phase of the heat pump, the mixing valve is fully closed and water is recirculated in a loop until the setpoint temperature is reached. The control of the storage temperature is performed by means of a temperature sensor coupled to a hysteresis control with a control band of 2 K. The temperature sensor is positioned at 1/3 of the total height of the storage tank.

Two different user tapping profiles were simulated based on profile "M" according to the standard EN 16147, which corresponds to an average consumption of a 4 person household. In the first ("M" standard) profile, the two major tappings (10 l/min) happen at 07:15 and 21:30 in the evening, with smaller tappings around noon (4 l/min) and at 20:30 (10 l/min). In the second ("M" modified) profile, domestic hot water is needed predominantly in the morning, with the two highest tappings taking place at 07:15 and 07:30. Smaller tappings happen also here at 12:45 and 20:30. The smallest tappings are equivalent to a volume flow of 4 l/min.

The mass flow of the distribution pump of the freshwater station is controlled by a PI controller while the user profile is taken into account by energy control. As soon as the desired hot water temperature is reached by the user (45°C), the energy control starts counting. Tapping continues until the desired energy has been supplied.

Laboratory testing

Firstly, the electric power consumption and the sound power level of radial and axial fans was evaluated in the acoustical testing laboratory to support design decision and to understand which effect has pressure drop on both these parameters. Secondly, a functional model of the façade-integrated heat pump was realised and measured in the laboratory to assess the real performance and compare it with simulation results. The performance of the refrigerant cycle was evaluated at 5, 10, 15 and 20 °C air inlet temperature and 30, 40 and 50 °C water supply temperature, thus investigating also the possibility of supplying low-temperature space heating. Sound power level measurements were also performed on the mock-up of façade-integrated outdoor unit.

Analysis and discussion of results

CFD-based optimization

The CFD-based outdoor unit development yielded the design in Figure 3. The final design involves thus four parallel axial fans and an evaporator, tilted of about 30° compared to the inflow direction. Table 2 summarizes the results obtained for the presented design. The choice of axial fans inspite of radial ones was supported by the measurements of the electrical power consumption and the sound power level, which will be presented in a later section.

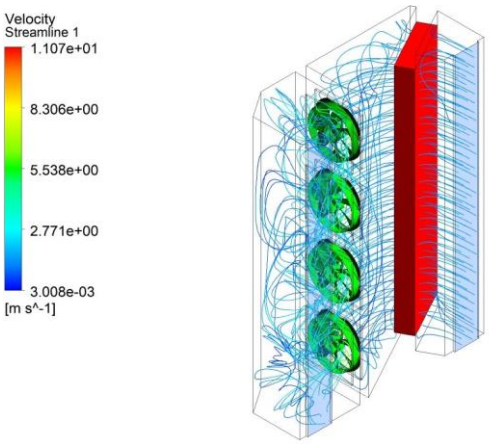

Figure 3: Final design of the outdoor element housing the evaporator and four axial fans and flow pattern simulated within the CFD environment.

Table 2: Results of the CFD simulation obtained for the presented design of the outdoor unit at the design air flow rate of 350 m^3/h.

Standard deviation (%)	15.2
Max. velocity (m/s)	1.2
Min. velocity (m/s)	0.5
Δp evaporator (Pa)	3.8
Δp evaporator + inflow (Pa)	4.2

Refrigerant cycle simulation

The simulation of the refrigerant cycle provided the performance maps depicted in Figure 4 to Figure 5. Performance data were thus generated for source temperatures between 5 °C and 20 °C as well as water

supply temperatures of 30, 40 and 50 °C. At 5 °C inlet air temperature and 50 °C supply water temperature, the heat pump is able to deliver about 1.4 kW of heating power, while at the same time the compressor exhibits an electric power consumption of about 0.6 kW. This would yield a COP, in this condition, equal to 2.3. These data will serve as an input in the dynamic system simulation and will be then compared to full-scale laboratory measurements.

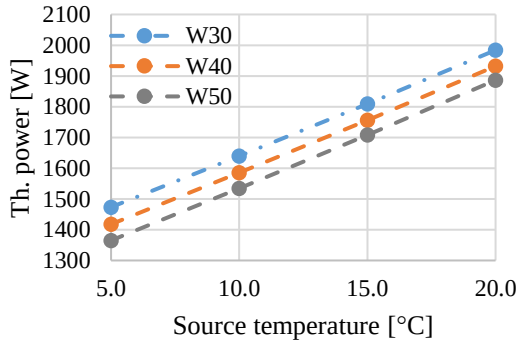

Figure 4: Performance map of the heating power depending from source temperature and water supply temperature.

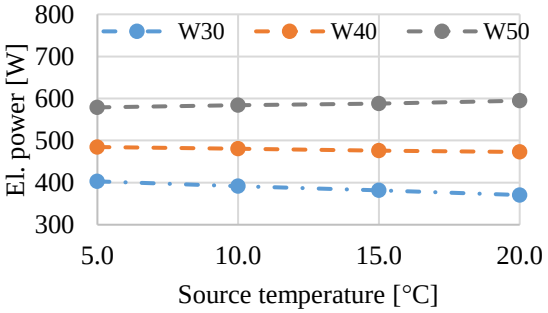

Figure 5: Performance map of the electric power consumption of the compressor depending from source temperature and water supply temperature.

Dynamic system simulation

Table 3 shows the results of the dynamic system simulation for the described hydraulic system assuming a "M Standard" tapping profile and a storage size of 90 liters. The seasonal performance factor for the simulated cases is defined as the ratio between the energy supplied by the heat pump to cover the DHW demand and eventual storage losses and the energy necessary to run the compressor. Thus the analysis does not include the electric consumption of eventual auxiliaries (e.g. circulating pumps, controls, etc.). The results for the remaining storage volumes of 100, 110 and 120 liters did not show a particular difference and, for each case, the heat pump was able to charge the hot water storage to the setpoint temperature in time for the tapping. For this reason, they were not reported here. Additionally, since no relevant difference could be pointed out among the different storage volumes, a compact 90 liters storage tank would be sufficient to guarantee adequate comfort conditions and easier installation.

Table 3: Results of the dynamic system simulation for a storage size of 90 liters depending on the outdoor air temperature.

ϑ_{src}	$W_{HP,el}$	Q_{DHW}	SPF
[°C]	[kWh]	[kWh]	[-]
-10	4.80	5.85	1.22
-7	4.35		1.34
2	3.44		1.70
7	3.10		1.89
12	2.80		2.08
20	2.45		2.38

If instead a "M modified" tapping profile is adopted and a storage volume of 90 liters is assumed, the heat pump is not able to fulfill, for outdoor air temperatures lower than 2 °C, the domestic hot water demand. In this case, storage sizes higher than 100 liters would be necessary to comply with the user demand and ensure an additional reserve capacity. For the Innsbruck climate a seasonal performance factor of 2.09 is expected (not considering the electrical power consumption attributed to deicing and auxiliaries).

Laboratory measurements

Figure 6 shows the measured sound power levels (A-corrected) for 4 axial fans or 1 single radial fan, depending on an imposed pressure drop upstream (by means of a ventilation flap). The measurements show thus that axial fans might be more favourable, in terms of acoustical emissions, with respect to radial fans if the pressure drop upstream of the fans can be contained below 20 Pa.

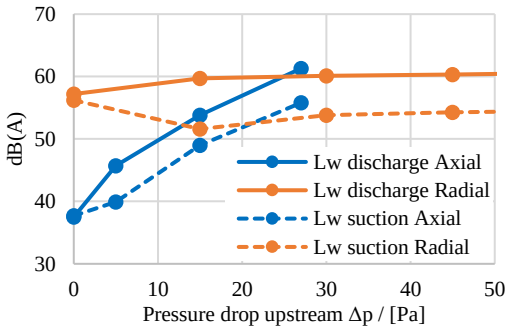

Figure 6: Measures sound power levels (A-corrected) on discharge and suction sides for 4 axial fans and 1 single radial fan at 350 m^3/h.

Additionally, the measured electric power consumption of axial fans was always much lower than radial fans.

Finally, the measurements performed on the functional unit of the heat pump yielded the results represented in Figure 7 and Figure 8, respectively for

the heating power and the electric power consumption. The measurements show generally a good agreement between measurements and simulation results. Deviations were observed in the electric power consumption for source temperatures lower or equal than 10 °C. This can be justified by the modelling assumption of a constant electrical efficiency, instead of adopting a more detailed function depending on evaporation and condensation temperatures. Finally the measurement of the sound power level of the façade-integrated mock-up yielded a sound power level of 42 dB(A) for the design air volume flow, due also to extensive adoption of sound absorbers.

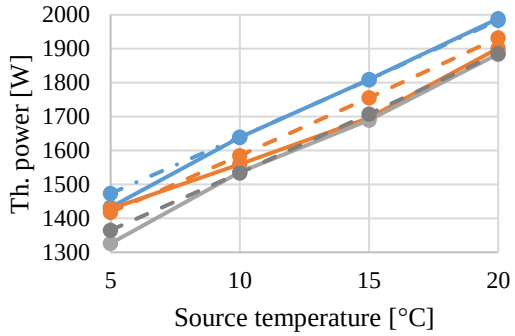

Figure 7: Measurement results (solid line) of the heating power for the tested functional model and comparison with simulated parameters (dotted line).

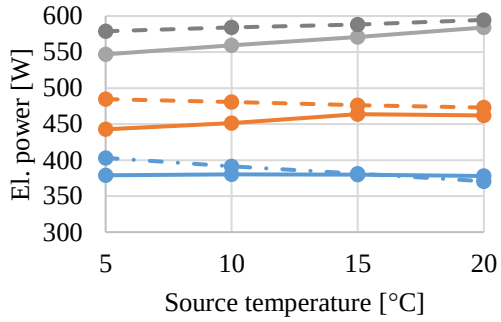

Figure 8: Measurement results (solid line) of the electric power consumption for the tested functional model and comparison with simulated parameters (dotted line).

Summary

A functional model of a mini-split air-to-water heat pump was developped by means of joint simulation and laboratory work. It can be concluded that a compact 90 liters storage tank would be sufficient to guarantee adequate comfort condition and fulfill user's needs, assumed that a tapping profile similar to the presented "M standard" is adopted. In the case where two major tappings take place one after the other (such as in the "M modified" profile), a volume of at least 110 liters would be necessary to meet the domestic hot water and comfort demands. A SPF of about 2.1 was obtained in the dynamic simulations. In the future the goal will be to improve it to at least a value of 2.5. A full-scale test with intermittent tapping will be performed in the upcoming weeks to verify the results obtained with the dynamic system simulation.

References

Abeykoon, C. (2020) 'Compact heat exchangers – Design and optimization with CFD', *International Journal of Heat and Mass Transfer*, 146, p. 118766. doi: 10.1016/j.ijheatmasstransfer.2019.118766.

DIN EN 14511-2 (2018) *Air conditioners, liquid chilling packages and heat pumps for space heating and cooling and process chillers, with electrically driven compressors - Part 2: Test conditions*.

DIN EN 16147 (2017) *Heat pumps with electrically driven compressors - Testing, performance rating and requirements for marking of domestic hot water units*. doi: https://dx.doi.org/10.31030/2513808.

Environmental Coalition on Standards (2021) 'Member States' ambition to phase out fossil-fuel heating – an analysis', (July). Available at: https://www.coolproducts.eu/wp-content/uploads/2021/07/ECOS-Coolproducts-Background-Briefing-MS-ambition-to-phase-out-fossil-fuel-heating.pdf.

European Commission (2018) 'Directive (EU) 2018/844 of the European Parliament and of the Council of 30 May 2018 amending Directive 2010/31/EU on the energy performance of buildings and Directive 2012/27/EU on energy efficiency', *Official Journal of the European Union*, 156(75), pp. 1–17. Available at: https://eur-lex.europa.eu/legal-content/EN/TXT/PDF/?uri=CELEX:32018L0844&from=EN.

European Commission (2019) 'Clean energy for all Europeans', p. 24. doi: 10.2833/9937.

IEA (2020) 'Austria 2020: Energy Policy Overview', *International Energy Agency*. Available at: https://www.iea.org/reports/austria-2020.

IEA (2021a) *Energy efficiency 2021*. Paris. Available at: https://www.iea.org/reports/energy-efficiency-2021.

IEA (2021b) 'Net Zero by 2050: A Roadmap for the Global Energy Sector'. Available at: https://iea.blob.core.windows.net/assets/deebef5d-0c34-4539-9d0c-10b13d840027/NetZeroby2050-ARoadmapfortheGlobalEnergySector_CORR.pdf.

Solar-Institut Juelich FH Aachen (2018) 'CARNOT Toolbox'. Available at: https://fh-aachen.sciebo.de/index.php/s/0hxub0iIJrui3ED.